frontiers in Marine Science

ORIGINAL RESEARCH
published: 19 November 2019
doi: 10.3389/fmars.2019.00699

Linking Internal Carbonate Chemistry Regulation and Calcification in Corals Growing at a Mediterranean CO_2 Vent

Marlene Wall[1,2†], Fiorella Prada[3†], Jan Fietzke[1], Erik Caroselli[3], Zvy Dubinsky[4], Leonardo Brizi[5], Paola Fantazzini[5], Silvia Franzellitti[6], Tali Mass[7], Paolo Montagna[8,9], Giuseppe Falini[10] and Stefano Goffredo[3*]*

[1] Marine Geosystems, GEOMAR Helmholtz-Centre for Ocean Research Kiel, Kiel, Germany, [2] Marine Benthic Ecology, GEOMAR Helmholtz-Centre for Ocean Research Kiel, Kiel, Germany, [3] Marine Science Group, Department of Biological, Geological, and Environmental Sciences, University of Bologna, Bologna, Italy, [4] The Mina and Everard Goodman Faculty of Life Sciences, Bar-Ilan University, Ramat Gan, Israel, [5] Department of Physics and Astronomy, University of Bologna, Bologna, Italy, [6] Animal and Environmental Physiology Laboratory, Department of Biological, Geological, and Environmental Sciences, University of Bologna, Ravenna, Italy, [7] Department of Marine Biology, Leon H. Charney School of Marine Sciences, University of Haifa, Haifa, Israel, [8] Institute of Marine Science ISMAR, National Research Council, Bologna, Italy, [9] Laboratoire des Sciences du Climat et de l'Environnement, Gif-sur-Yvette, France, [10] Department of Chemistry "Giacomo Ciamician", University of Bologna, Bologna, Italy

OPEN ACCESS

Edited by:
Marius Nils Müller, Federal University of Pernambuco, Brazil

Reviewed by:
Wei-dong Zhai, Shandong University, China
Hongjie Wang, University of Delaware, United States
Claire Ross, Department of Biodiversity, Conservation and Attractions (DBCA), Australia

***Correspondence:**
Marlene Wall
mwall@geomar.de
Stefano Goffredo
s.goffredo@unibo.it

† These authors have contributed equally to this work

Specialty section:
This article was submitted to Marine Biogeochemistry, a section of the journal Frontiers in Marine Science

Received: *03 June 2019*
Accepted: *31 October 2019*
Published: *19 November 2019*

Citation:
Wall M, Prada F, Fietzke J, Caroselli E, Dubinsky Z, Brizi L, Fantazzini P, Franzellitti S, Mass T, Montagna P, Falini G and Goffredo S (2019) Linking Internal Carbonate Chemistry Regulation and Calcification in Corals Growing at a Mediterranean CO_2 Vent. Front. Mar. Sci. 6:699. doi: 10.3389/fmars.2019.00699

Corals exert a strong biological control over their calcification processes, but there is a lack of knowledge on their capability of long-term acclimatization to ocean acidification (OA). We used a dual geochemical proxy approach to estimate the calcifying fluid pH (pH_{cf}) and carbonate chemistry of a Mediterranean coral (*Balanophyllia europaea*) naturally growing along a pH gradient (range: pH_{TS} 8.07–7.74). The pH_{cf} derived from skeletal boron isotopic composition ($\delta^{11}B$) was 0.3–0.6 units above seawater values and homogeneous along the gradient (mean ± SEM: Site 1 = 8.39 ± 0.03, Site 2 = 8.34 ± 0.03, Site 3 = 8.34 ± 0.02). Also carbonate ion concentration derived from B/Ca was homogeneous [mean ± SEM (μmol kg^{-1}): Site 1 = 579 ± 34, Site 2 = 541 ± 27, Site 3 = 568 ± 30] regardless of seawater pH. Furthermore, gross calcification rate (GCR, mass of $CaCO_3$ deposited on the skeletal unit area per unit of time), estimated by a "bio-inorganic model" (lpHRAC), was homogeneous with decreasing pH. The homogeneous GCR, internal pH and carbonate chemistry confirm that the features of the "building blocks" – the fundamental structural components – produced by the biomineralization process were substantially unaffected by increased acidification. Furthermore, the pH up-regulation observed in this study could potentially explain the previous hypothesis that less "building blocks" are produced with increasing acidification ultimately leading to increased skeletal porosity and to reduced net calcification rate computed by including the total volume of the pore space. In fact, assuming that the available energy at the three sites is the same, this energy at the low pH sites could be partitioned among fewer calicoblastic cells that consume more energy given the larger difference between external and internal pH compared to the control, leading to the production of less building blocks (i.e., formation of pores inside the

skeleton structure, determining increased porosity). However, we cannot exclude that also dissolution may play a role in increasing porosity. Thus, the ability of scleractinian corals to maintain elevated pH_{cf} relative to ambient seawater might not always be sufficient to counteract declines in net calcification under OA scenarios.

Keywords: pH up-regulation, ocean acidification, *Balanophyllia europaea*, Mediterranean Sea, boron, calcifying fluid, carbonate chemistry

INTRODUCTION

Changing ocean pH and carbonate chemistry due to increasing atmospheric carbon dioxide, a phenomenon known as ocean acidification (OA), has multiple effects on marine organisms, for example on fish reproduction (Miller et al., 2013), on the formation of invertebrate skeletal structures (Ries et al., 2009), on macro-algae abundance (Connell and Russell, 2010), with the majority of studies showing negative responses (Fabry et al., 2008; Goffredo et al., 2014), including dissolution of reef sediments which may respond even more rapidly to OA than coral calcification (Eyre et al., 2018). Calcifying organisms are expected to be particularly sensitive to the effects of OA. Many investigations documented reductions in calcification rates of shellfish (Gazeau et al., 2013), shell-forming marine plankton (Beaufort et al., 2011), and reef-building corals (De'ath et al., 2009; Fabricius et al., 2011) caused by the seawater pH-dependent reduced concentrations of carbonate ions ($[CO_3^{2-}]$) used by these organisms to form their mineralized structure.

In scleractinian corals, calcification is thought to occur within a physiologically controlled calcifying fluid (cf) in a semi-confined environment between the coral skeleton and its calicoblastic cell layer (McCulloch et al., 2012a; Ohno et al., 2017; Sevilgen et al., 2019). Carbonate chemistry of the calcifying fluid is exquisitely regulated through cellular mechanisms that aid in shifting the equilibrium composition of dissolved inorganic carbon (DIC) in favor of CO_3^{2-} relative to bicarbonate ions (HCO_3^-), increasing the pH_{cf} and saturation state (Ω_{cf}) to promote the precipitation of calcium carbonate and skeletal growth (Zoccola et al., 2015). The degree of control over Ω_{cf} is crucial to determine relative sensitivities toward changes in seawater pH and other adverse environmental conditions (Cohen and Holcomb, 2009; McCulloch et al., 2012a). Alternatively, a recent study on *Stylophora pistillata* demonstrated the occurrence of amorphous calcium carbonate (ACC) precursor nanoparticles formed within the animal tissue (Mass et al., 2017). These nanoparticles precipitate inside vesicles formed by endocytosis of seawater by the cell membrane and are subsequently transported to the surface of coral skeletons, where ACC crystallizes into aragonite (Mass et al., 2017). The vesicles may be the site where the calcifying fluid resides (Mass et al., 2017).

The boron isotopic proxy method ($\delta^{11}B$) (Trotter et al., 2011) and the B/Ca method (Holcomb et al., 2016; McCulloch et al., 2017) can be applied to estimate pH_{cf}, $[CO_3^{2-}]_{cf}$ and DIC_{cf} at the time of skeleton deposition. The underlying chemical principle is based on the pH-dependency of boron speciation in seawater between boric acid, $B(OH)_3$, and borate ion, $B(OH)_4^-$, on the isotopic fractionation associated with this speciation (Klochko et al., 2006), and on the assumption that only borate ions are incorporated into the carbonate skeleton (Hemming and Hanson, 1992). From skeletal boron isotope fraction ($\delta^{11}B$), it is possible to infer the pH at the calcification site (Hönisch et al., 2004; Krief et al., 2010; McCulloch et al., 2012a, 2018), which does not necessarily match that of seawater. The B/Ca ratio depends inversely on the concentration of carbonate ions ($[CO_3^{2-}]$), since borate substitutes carbonate ions into the aragonite lattice (Holcomb et al., 2016). The validity of B/Ca as a proxy for coral $[CO_3^{2-}]_{cf}$ has been demonstrated by comparing geochemically derived values of inorganic aragonite precipitation from solutions at known $[CO_3^{2-}]_{cf}$ (Holcomb et al., 2016). Direct measurements support $[CO_3^{2-}]_{cf}$ up-regulation (Cai et al., 2016; Sevilgen et al., 2019). Calcification rates have been inferred from these proxies using modeling approaches that have been successfully employed in studies with tropical corals (McCulloch et al., 2012a; Wall et al., 2016; Comeau et al., 2017a,b). Yet we also need to consider that these models assume constant calcium ion concentrations. Recent studies found changes in internal Ω_{cf} through Raman spectroscopy (DeCarlo et al., 2017) and linked this to potential changes in calcium concentrations at the site of calcification further highlighting the role of calcium regulation in calcification (DeCarlo et al., 2018).

Different definitions of calcification and calcification rates exist in the literature, depending on whether the effect of dissolution is considered in the models. Generally speaking, it is assumed that the net calcification rate (NCR) corresponds to gross calcification rate (GCR) minus dissolution (D) (Andersson and Mackenzie, 2012; Cohen and Fine, 2012; Comeau et al., 2014). NCR is directly measured in living corals by buoyant weight and total alkalinity techniques (Smith and Key, 1975; Bucher et al., 1998). GCRs are derived from the evaluation of ^{45}Ca incorporation to the coral skeleton (Cohen and Fine, 2012; Cohen et al., 2017). Inconsistencies on the responses of calcifying marine species to OA reported in several studies could be due to how NCR is related to GCR and D (Cohen and Fine, 2012). First, it is worth noting that to transform this qualitative relationship into the simple equation NCR = GCR-D some caution is needed. The measurements of NCR and GCR have to be related to the same period of growth, an important parameter in the definition of both measurements (Rodolfo-Metalpa et al., 2011). Moreover, because GCRs are generally obtained as the evaluation of deposited $CaCO_3$ per surface unit, it is straightforward that NCR should be evaluated as a density × linear extension rate, that allows a direct comparison of these parameters (Tortolero-Langarica et al., 2017). In addition, it is not sufficient that all the three parameters are described with the same units [as mass of $CaCO_3$ deposited (or loss, in the case of D) on the skeletal unit

area per unit of time], it is necessary that these three parameters refer also to the same components of the coral skeleton, with particular attention to the fact that the coral skeleton is made of the solid matrix and the voids (the pore spaces).

In this study, for the first time, skeletal $\delta^{11}B$ and B/Ca proxies were employed to infer changes of pH_{cf}, $[CO_3^{2-}]_{cf}$, and DIC_{cf} in a Mediterranean scleractinian coral, *Balanophyllia europaea*, living along a natural pH gradient at the volcanic seep of Panarea (Italy). Results were further used to compute carbonate chemistry based Ω_{cf} and GCRs at the different pH conditions, and to compare the obtained data with data on NCR, linear extension and structural features at the micro and macro-scale previously measured in the same corals (Goffredo et al., 2014; Fantazzini et al., 2015). The whole approach disclosed the homeostatic capability of *B. europaea,* here selected as a model species for temperate scleractinian corals, toward pH and carbonate chemistry at the site of calcification.

MATERIALS AND METHODS

Coral Samples

Twenty specimens of the scleractinian zooxanthellate coral *B. europaea* were collected between November 2010 and May 2013 from three sites (6–7 individuals per site) along a pH gradient at a CO_2 seep near Panarea Island (Italy) (**Figure 1**). This underwater crater 20 × 14 m wide and 10 m deep generates hydrothermally stable CO_2 emissions that generate a pH gradient at ambient temperature. In particular, sampling sites, whose seawater physic-chemical parameters have been previously characterized from 2010 to 2013 (Goffredo et al., 2014; Fantazzini et al., 2015; Prada et al., 2017), were selected to closely match pH values projected for 2100 under different IPCC scenarios (IPCC, 2014): average pH_{TS} = 8.07 (Site 1: present-day conditions), average pH_{TS} = 7.87 (Site 2: RCP6), average pH_{TS} = 7.74 (Site 3: RCP8.5). Temperature, salinity and pH_{NBS} were measured in a previous study (Prada et al., 2017) with a multi-parametric probe (600R, YSI Incorporated) powered from a small boat and operated by SCUBA divers. In the same study, the measured pH_{NBS} were converted to the total scale using CO2SYS software. The pH_{TS}, total alkalinity, salinity, and temperature were then used to calculate aragonite saturation and the other carbonate system parameters using the software CO2SYS (Prada et al., 2017), although the CO_2 vent may alter the composition of major ions.

After coral collection, skeletons were cleaned with 1% sodium hypochlorite solution for 3 days to dissolve polyp tissue. After washing with deionized water and drying at 50°C for 3–4 days, each coral was examined under a binocular microscope to remove any visible contamination and encrusting organisms (Caroselli et al., 2011).

Sample Preparation, $\delta^{11}B$ and B/Ca Determination

Collected corals were embedded in resin, cut in half and the surface polished. The $\delta^{11}B$ and B/Ca composition was measured simultaneous by laser ablation multi collector inductive coupled plasma mass spectrometer (Thermo Fisher MC-ICP-MS AXIOM, connected to a UP193fx laser ablation system of New Wave Research, equipped with an excimer 193 nm laser). The measurement procedure used standard methods (Fietzke et al., 2010; Wall et al., 2016) with slight modifications. In this study, multiplier and Faraday cups were used simultaneously to collect data for ^{10}B and ^{11}B (both on multiplier) as well as ^{12}C (Faraday cup). The cones were cleaned on a regular basis (every 2–4 days). The tubes going from the ablation cell to the plasma torch were checked for material deposition and cleaned by high flow rates overnight and/or mobilization of the debris by increased flow rates transporting it out of the tubes. Prior to each measurement session the standard and samples were pre-ablated to remove surface contaminations using a laser spot diameter of 50 μm (double the size of the actual measurement spot). A standard-sample-bracketing method was used. The data of one measurement session contained 5–6 brackets. Both ^{12}C and the variation of the standard (NIST SMR610) for each session were used to check for instrument stability and contaminations. Sessions were repeated when the standard drift was higher than the internal reproducibility of the standards (2SD of the session on the standards). Twenty individual laser tracks (25 × 500 μm) were performed (ablating consecutively each transect 10 × with 10 μm s^{-1} and 10 Hz) along the oral-aboral axis of the corallite (i.e., to represent calcifying fluid pH, carbonate chemistry, and growth rates of the entire coral) as close as possible to the edge of the skeletal section (expecting to mainly ablate fibers and avoid centers of calcification, COC), far enough away to avoid ablation through the skeletal structure into the pore space. Yet COC areas may not have been completely avoided. To account for this we: a) subsequently screened the individual tracks for anomalous ^{12}C values indicative of either ablation through the coral skeletal structure (the coral skeleton is not massive but consists of pores; cutting the coral and ablating from a cross section we cannot tell from the top-view the depth of the underlying skeletal structure, thus this screening is done afterward) or increased organics (potentially reflecting COC) and excluded this parts from analysis, and b) aimed for 20 tracks of approximately 25 × 500 × 20 μm on all individuals to have a representative $\delta^{11}B$ dataset per individual and by this we expect the error to be similar among corals (assuming that COC to fiber ratio in coral grown under various environmental conditions stays constant). The transects were positioned to encompass the entire coral cut along their growth axis from close to the base up to the tips of the cut skeletal structures to obtain a representative data set per sample. The data reduction followed Fietzke et al., 2010. For each individual $\delta^{11}B$ transect, an average instrumental precision of <0.8‰ (±1 SD) for approx. 1.7 μg of carbonate sample was achieved. The dataset reflects the high variability in $\delta^{11}B$ for a single coral, and all transects per coral were averaged afterward to yield values that reflect the average $\delta^{11}B$, pH_{cf}, and ΔpH at each seawater pH_{TS} condition (see below).

B/Ca data are based on the integrated boron intensities (^{10}B + ^{11}B) divided by the ^{12}C intensity. The calibration (conversion from intensity ratios to concentration ratios) has been done using a *Lophelia pertusa* cold-water coral sample covering a B/Ca range of about 450–950 μmol/mol, which had

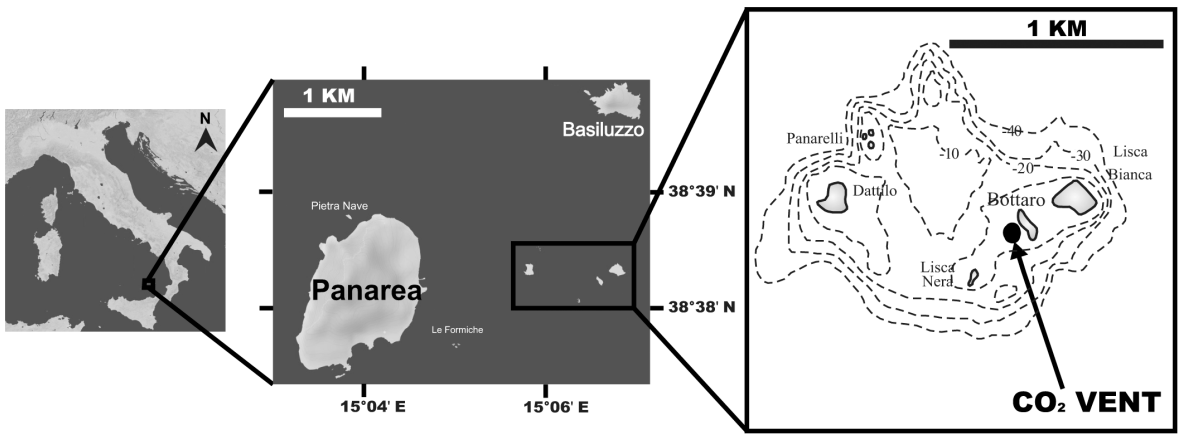

FIGURE 1 | Map of the study site off Panarea Island (Aeolian Archipelago, Italy); insets show the location of the vent area, SE of Bottaro, where corals were collected. Maps were generated using d-maps (www.d-maps.com).

been determined before using LA-ICP-MS relative to standard NIST-SRM610 using ^{43}Ca as internal standard. This calibration procedure resulted in: B/C [μmol/mol] = 78800 × B/C [cps/cps]; (cps – counts per second, ion beam intensity). We used stoichiometric ratio of C/Ca = 1 as approximation for natural carbonates and translated B/C ratios in B/Ca [μmol/mol] ratios.

pH_{cf} Calculations

Each $\delta^{11}B$ value was converted into pH of the calcifying fluid (pH_{cf}) following eq. 1 (McCulloch et al., 2012b) with a seawater $\delta^{11}B_{sw}$ of 39.61‰ (Foster et al., 2010), a fractionation factor (α_B) of 1.0272 (Klochko et al., 2006) and pK^*_B of 8.640 at Site 1 with an average temperature of 20.5°C, 8.637 for Site 2 with an average temperature of 20.7°C and 8.638 at Site 3 with a temperature of 20.6°C (salinity at all site is 37).

$$pH_{cf} = pK_B^* - \log\left[\frac{\delta^{11}B_{sw} - \delta^{11}B_c}{\alpha_B \times \delta^{11}B_c - \delta^{11}B_{sw} + 1000 \times (\alpha_B - 1)}\right] \quad \text{(Trotter et al., 2011)} \quad (1)$$

Since our study aims to derive calcifying fluid pH and not seawater pH, $\delta^{11}B_{sw}$ is replaced by $\delta^{11}B_{cf}$. $\delta^{11}B_c$ is the isotope value of the corals. As generally assumed, we have used the values of the seawater because seawater is transported to the site of calcification, located between the base of the calicoblastic epithelium and the existing skeletal surface (Gagnon et al., 2012). Following the method in Trotter et al. (2011) the superimposed physiological pH control was calculated with the equation:

$$\Delta pH = pH_{cf} - pH_{TS} \quad (2)$$

and related to the seawater pH_{TS} to quantify the extent of the physiological control on the internal pH_{cf}.

$[CO_3^{2-}]_{cf}$ and DIC_{cf} Calculations

Skeletal B/Ca data were used to assess $[CO_3^{2-}]_{cf}$ based on recently established relationship between the concentrations of borate and carbonate ions in the solution from which aragonite is precipitated (Holcomb et al., 2016):

$$[CO_3{}^{2-}]_{cf} = [B(OH)_4^-]_{cf} \times K_D{}^{B/Ca}/(B/Ca) \quad (3)$$

Where $[B(OH)_4^-]_{cf}$ is the pH-dependent borate concentration derived from $\delta^{11}B$, B/Ca is the ratio measured in the coral skeleton and $K_D{}^{B/Ca}$ is the distribution coefficient for boron between the aragonite and seawater, refit as a function of $[H^+]$[45]:

$$K_D{}^{B/Ca} = 0.00297exp(-0.0202[H^+]_{cf}) \quad (4)$$

The hydrogen ion concentration of the calcifying fluid was calculated from the $\delta^{11}B$-derived pH_{cf}. To estimate $[B(OH)^-{}_4]_{cf}$, we assume total boron at the site of calcification equals seawater concentration and depends only on seawater salinity.

Both pH_{cf} and $[CO_3{}^{2-}]_{cf}$ were then used to calculate DIC_{cf} using the R seacarb package with carbonic acid dissociation constants (K1, K2) (Millero et al., 2006) and stability constant of hydrogen sulfate (ks) (Dickson, 1990). DIC_{cf} up-regulation within the calcifying fluid was calculated as the DIC_{cf}/DIC_{sw} ratio.

Gross Calcification Rate (GCR) and Calcification Site Conditions

Boron-derived internal pH_{cf} was used to calculate GCR. We used the IpHRAC model (McCulloch et al., 2012a):

$$GCR = k \times (\Omega_{cf} - 1)^n \quad (5)$$

Where k is the temperature-dependent rate law constant, n is the order of the reaction and Ω_{cf} is the aragonite saturation state of the calcifying fluid, which was calculated using seacarb from pH_{cf} and DIC_{cf} (using the same constants for calculation as above). We assumed $[Ca]^{2+}$ concentration equal to seawater concentration with average salinity of 37. The modeled GCR was calculated for average temperature (t) per site with k and n for aragonite precipitation (Burton and Walter, 1987):

$$k = -0.0177 \times t^2 + 1.47 \times t + 14.9 \quad (6)$$

$$n = 0.0628 \times t + 0.0985. \quad (7)$$

This model only requires the knowledge of internal pH_{cf} and DIC_{cf} or ${CO_3}^{2-}{}_{cf}$ and does not account for changes in energy investment due to changes in proton removal rate. In general, internal pH_{cf} is not only a matter of the intensity of up-regulation (proton removal rate) but also influenced by the rate of calcification. Calcification is a process that produces protons ($Ca^{2+} + HCO_3^- \Leftrightarrow CaCO_3 + H^+$) (Allemand et al., 2004), which need to be removed from the site of calcification. Calcification and proton removal are processes that influence calcifying fluid equilibrium and pH_{cf} levels.

Net Calcification Rates

The mean annual NCR (mass of $CaCO_3$ deposited per year per area unit) was calculated for each specimen by applying the following formula: calcification (mg mm^{-2} $year^{-1}$) = skeletal density (mg mm^{-3}) × linear extension (mm $year^{-1}$) (Lough and Barnes, 2000; Carricart-Ganivet, 2004). Corallite length (L: maximum axis of the oral disc), width (W: minimum axis of the oral disc) and height (h: oral-aboral axis) were measured with calipers and the dry skeletal mass (M) was measured with a precision balance. Corallite volume was calculated using the formula: $V = L^2 \times W^2 \times h\pi$ (Caroselli et al., 2019). The skeletal density for each corallite was calculated as M/V and the linear extension as L/age. The age of each specimen was estimated by applying the Von Bertalanffy growth function, using the asymptotic length and growth constants for *B. europaea* along the Panarea pH gradient (Caroselli et al., 2019).

If the density considered is the bulk density, which is the mass divided by the total enclosed volume, including the volume of the enclosed skeletal voids (i.e., the volume of the pore space inside the skeleton), the resulting NCR may be called "bulk-NCR," i.e., the parameter refers to an average calcification on the apparent volume of the whole sample, including the skeletal pores. If the density considered is the skeletal biomineral density (i.e., micro-density; Caroselli et al., 2011), which is mass per unit volume of the material which composes the skeleton, NCR may be considered "micro-NCR," i.e., the parameter will refer to an average calcification over the volume of the solid skeleton matrix, thus excluding the pores. These definitions (i.e., micro-NCR and bulk-NCR) are used hereafter.

Statistical Analysis

One-way analysis of variance (ANOVA) was used to compare the geochemical values, the calcifying conditions, GCR, and bulk-/micro-NCR among sites. When assumptions for parametric statistics were not fulfilled, the non-parametric Kruskal–Wallis equality-of-populations rank test was used, including the Monte Carlo correction for small sample size (Gabriel and Lachenbruch, 1969). Spearman's rank correlation coefficient was used to calculate the significance of the correlations between seawater pH_{TS} with coral ΔpH and bulk-NCR. Statistical analyses were performed using SPSS 20.0 and data visualization was done with R Studio version 3.0.1 (R Core Team, 2015).

RESULTS

$\delta^{11}B$ and $\delta^{11}B$-Derived Calcifying Fluid pH and Carbonate Chemistry

The boron isotopic composition ($\delta^{11}B$) of *B. europaea* skeletons was assessed in corals sampled at three seawater pH levels (expressed in total scale, pH_{TS}) from three Sites along the Panarea gradient (Site 1: pH_{TS} = 8.07; Site 2 = 7.87; Site 3 = 7.74, **Supplementary Table 1**) (Goffredo et al., 2014). An average ∼1.7% coefficient of variation of $\delta^{11}B$ values within the same Site was observed (**Figure 2A**). No significant differences in average

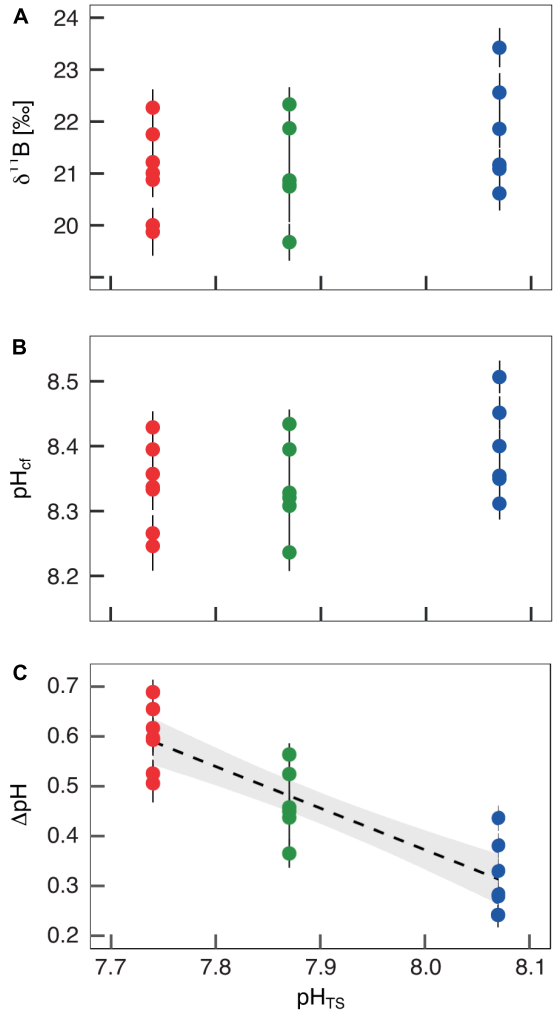

FIGURE 2 | Boron isotopic signature ($\delta^{11}B$), $\delta^{11}B$-derived pH in the calcifying fluid (pH_{cf}) and pH up-regulation (ΔpH) in *Balanophyllia europaea* along the pH_{TS} gradient at Panarea Island. **(A)** $\delta^{11}B$ measured in corals collected at three different sites along a natural pH gradient (Site 1, average pH_{TS} 8.07 = blue; Site 2, average pH_{TS} 7.87 = green; Site 3, average pH_{TS} 7.74 = red). From the boron isotopic signature **(B)** pH_{cf} and **(C)** ΔpH (pH_{cf} – pH_{TS}) were calculated. At each site, filled circles and error bars represent means ± SEM per coral. Black dashed line indicates linear regression and the gray area the 95%-CI band of the significant regression ($p < 0.001$; $N = 7$ for Sites 1 and 3, and $N = 6$ for Site 2).

$\delta^{11}B$ between the three Sites were observed (mean ± SEM (‰): Site 1 = 21.70 ± 0.37, Site 2 = 21.05 ± 0.38, Site 3 = 21.00 ± 0.33, $p > 0.05$; **Figure 2A**, **Supplementary Table 2**). Thus, on average, derived internal pH_{cf} values were homogeneous along the pH_{TS} gradient (mean ± SEM: Site 1 = 8.39 ± 0.03, Site 2 = 8.34 ± 0.03, Site 3 = 8.34 ± 0.02, $p > 0.05$; **Figure 2B**, **Supplementary Table 2**). Values of ΔpH ($pH_{cf} - pH_{TS}$) resulted significantly different among Sites (mean ± SEM: Site 1 = 0.32 ± 0.03, Site 2 = 0.47 ± 0.03, Site 3 = 0.60 ± 0.02, $p < 0.001$; **Figure 2C**, **Supplementary Table 2**) and negatively correlated with pH_{TS} ($r_s^2 = 0.78$, $p < 0.001$; **Figure 2C**). Similar to $\delta^{11}B$, no significant differences in B/Ca values were found between Sites [mean ± SEM (μmol mol^{-1}): Site 1 = 778 ± 38, Site 2 = 767 ± 32, Site 3 = 745 ± 25, $p > 0.05$; **Figure 3A**; **Supplementary Table 2**], resulting in homogenous $[CO_3^{2-}]_{cf}$ [mean ± SEM (μmol kg^{-1}): Site 1 = 579 ± 34, Site 2 = 541 ± 27, Site 3 = 568 ± 30, $p > 0.05$; **Figure 3B**; **Supplementary Table 2**], dissolved inorganic carbon concentrations (DIC_{cf}) [mean ± SEM (μmol kg^{-1}): Site 1 = 3050 ± 149, Site 2 = 3156 ± 160, Site 3 = 3305 ± 104, $p > 0.05$; **Figure 3C**] as well as DIC-ratio [DIC_{cf}/DIC_{sw}, **Supplementary Figure 1**].

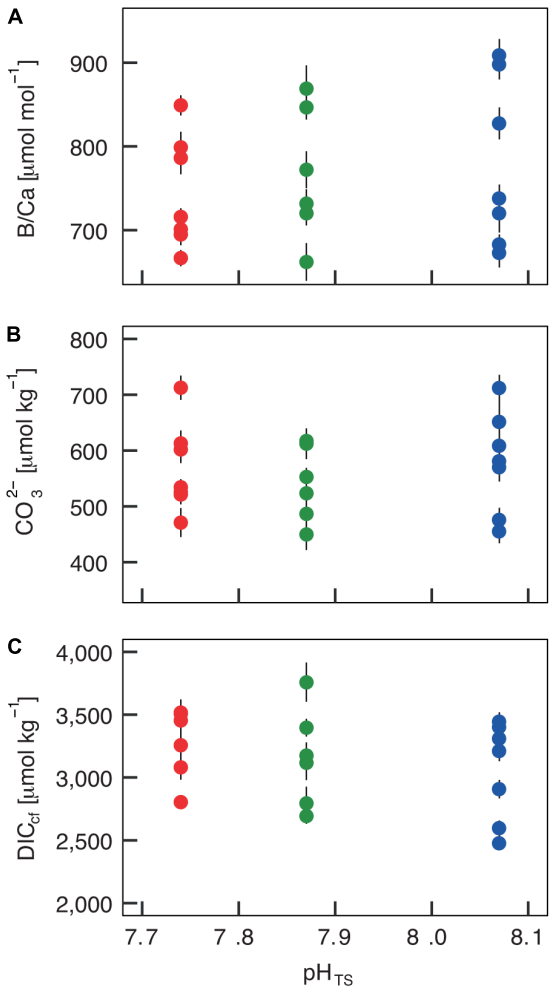

FIGURE 3 | Internal carbonate ion concentration ($[CO_3^{2-}]$) and dissolved inorganic carbon concentration (DIC_{cf}) at the calcification site derived from the skeletal B/Ca concentration in *Balanophyllia europaea* along the pH_{TS} gradient at Panarea Island, Italy. **(A)** Coral skeletal B/Ca ratio from naturally different seawater pH (pH in total scale) sites were translated into **(B)** internal calcifying fluid $[CO_3^{2-}]$ values and **(C)** DIC_{cf}. Circles represent values for each individual coral (mean ± SEM). Color denotes the different locations: Site 1 = blue, Site 2 = green, Site 3 = red.

Calcifying Fluid Aragonite Saturation State and Calcification Rates

Figures 4, **5** report the results from the bio-inorganic model (McCulloch et al., 2012a) that inferred Ω_{cf} values and GCRs. Calcifying fluid aragonite saturation state (Ω_{cf}) in *B. europaea* along the gradient showed no significant differences among Sites with values of 8.90 ± 1.40 (mean ± SEM) in Site 1, 8.31 ± 1.03 in Site 2, and 8.74 ± 1.23 in Site 3. GCRs also did not show significant differences among Sites, with relative values of 1.00 ± 0.09 in Site 1, 0.92 ± 0.07 in Site 2, 0.98 ± 0.08 in Site 3 (real values: 675 ± 63 μmol cm^{-2} h^{-1} in Site 1, 621 ± 49 μmol cm^{-2} h^{-1} in Site 2, 661 ± 55 μmol cm^{-2} h^{-1} in Site 3) (**Figures 4**, **5A**, **Supplementary Table 3**). Micro-NCR was also homogeneous among sites, with relative values of 1.00 ± 0.02 in Site 1, 0.97 ± 0.07 in Site 2, and 0.88 ± 0.05 in Site 3 (real values: 3.29 ± 0.07 mg mm^{-2} $year^{--1}$ in Site 1, 3.19 ± 0.23 mg mm^{-2} $year^{-1}$ in Site 2, and 2.89 ± 0.19 mg mm^{-2} $year^{-1}$ in Site 3) (**Figure 5B**, **Supplementary Table 3**) while bulk-NCR decreased significantly with decreasing pH_{TS} ($r = 0.586$, $p < 0.01$; **Figure 5C**) with relative values of 1.00 ± 2.29 in Site 1, 0.92 ± 0.07 in Site 2, and 0.84 ± 0.05 in Site 3 (real values: 2.29 ± 0.06 mg mm^{-2} $year^{-1}$ in Site 1, 2.10 ± 0.16 mg mm^{-2} $year^{-1}$ in Site 2, and 1.92 ± 0.11 mg mm^{-2} $year^{-1}$ in Site 3) (**Supplementary Table 3**). Micro- and bulk-NCR were calculated from previously reported micro-density, bulk density, and linear extension measurements (Fantazzini et al., 2015).

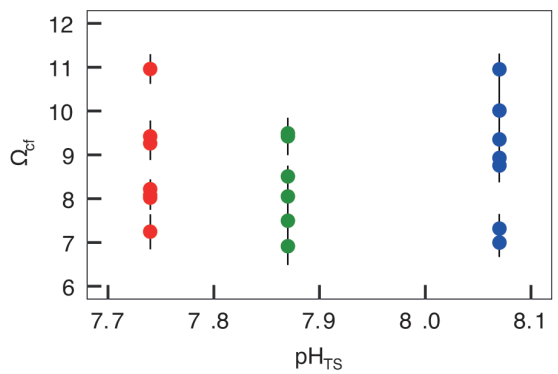

FIGURE 4 | Skeletal aragonite saturation state (Ω_{cf}) assessed in *Balanophyllia europaea* corals growing along the pH_{TS} gradient at Panarea Island. Ω_{cf} was calculated from the average internal pH_{cf} of the individual corals and the DIC_{cf} concentration. Circles represent values for each individual coral (mean ± SEM). Color denotes the different sampling sites: Site 1 = blue, Site 2 = green, Site 3 = red.

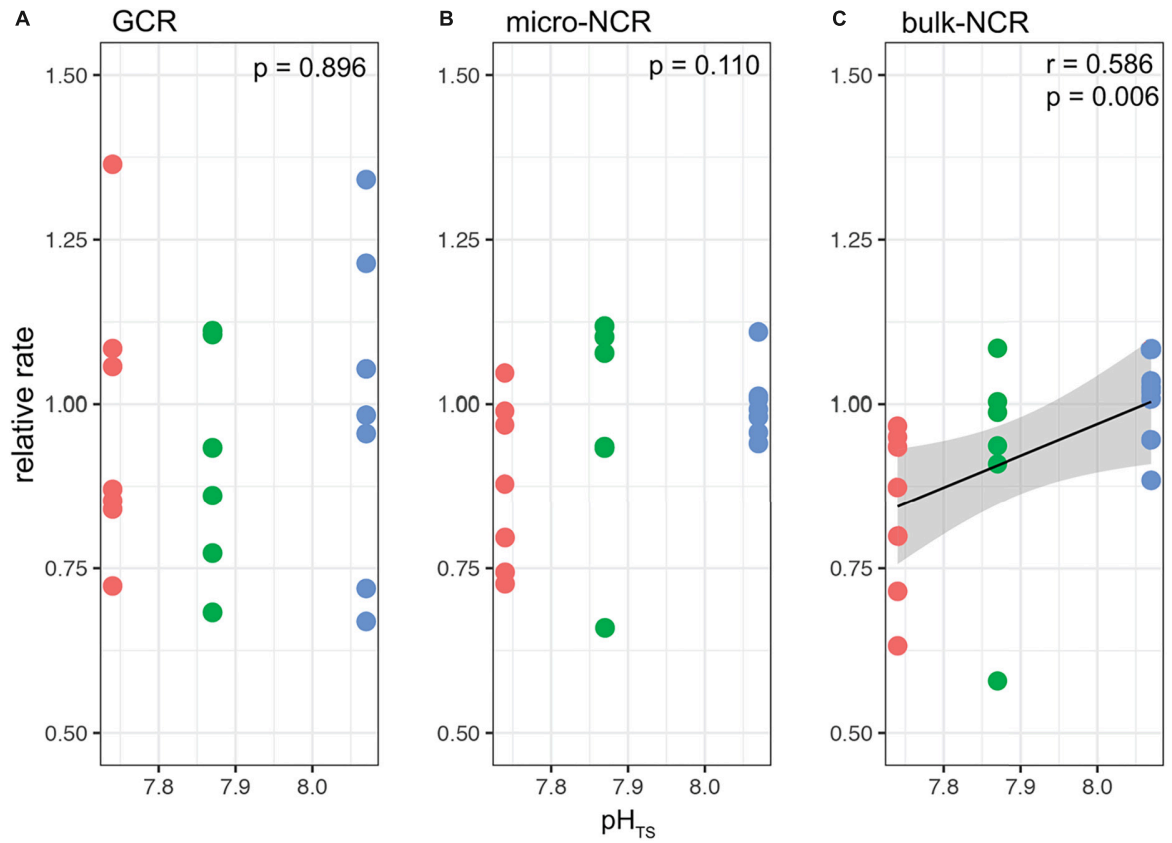

FIGURE 5 | Modeled gross calcification rates (GCR) and comparisons with measured micro and bulk net calcification rates (NCR) in *Balanophyllia europaea* corals growing along the pH_{TS} gradient at Panarea Island. **(A)** GCRs were calculated following the IpHRAC model (McCulloch et al., 2012a) (internal pH regulation and abiotic calcification): Gross calcification = $k \times (\Omega_{cf}-1)^n$ and presented as relative rates (setting average control growth as 1). **(B)** micro-NCR and **(C)** bulk-NCR were derived from bulk density, micro-density and linear extension rates taken from Fantazzini et al. (2015). Circles represent values for each individual coral. Color denotes the different locations: Site 1 = blue, Site 2 = green, Site 3 = red. Black dashed line indicates linear regression and the gray area the 95%-CI band of the significant regression ($p < 0.01$; $N = 7$ for Sites 1 and 3, and $N = 6$ for Site 2).

DISCUSSION

Structural analyses on *B. europaea* naturally living along the pH gradient of Panarea (Italy) display no significant change in mineralogy with decreasing pH (Goffredo et al., 2014). Analyses at the micro-scale level revealed no changes in skeletal micro-density (Fantazzini et al., 2015), calcium carbonate polymorph, organic matrix content, aragonite fiber thickness, and skeletal hardness in corals growing along the pH gradient (Goffredo et al., 2014). Nevertheless, at the macro-scale, reduction of NCRs (i.e., bulk-NCR, by using the bulk density in the definition of NCR) and parallel increases in skeletal porosity, coupled with a decrease in skeletal bulk density, are observed (Fantazzini et al., 2015), likely to keep unchanged linear extension rates and meet functional reproductive needs (e.g., the ability to reach critical size at sexual maturity and the reproductive output) (Fantazzini et al., 2015). A critical outcome is the reduced mechanical strength of the skeletons, increasing damage susceptibility, which was hypothesized to explain the decline of population density observed at low pH values (i.e., the species disappears at pH < 7.7) (Goffredo et al., 2014).

In order to determine the calcification conditions that promote the above described phenotypic outcomes and gain insights into the degree of biological control over these conditions exerted by *B. europaea*, this study employed a dual-geochemical proxy approach and assessed carbonate chemistry of the calcification fluids on a subsample of the same corals previously analyzed (Fantazzini et al., 2015).

$\delta^{11}B$ and $\delta^{11}B$-Derived Calcifying Fluid pH and Carbonate Chemistry

Up-regulation of pH_{cf}, DIC_{sw}, and Ω_{cf} above environmental values is a regulatory strategy adopted by many calcifying organisms, including corals, to maintain high concentrations of carbonate $[CO_3^{2-}]_{cf}$ and calcium $[Ca^{2+}]_{cf}$ ions in the calcifying fluids while eliminating H^+ end-products (Cai et al., 2016; Ramesh et al., 2017; Ross et al., 2019; Sevilgen et al., 2019), hence promoting biomineral precipitation and maintaining physiological calcification rates. Specimens sampled at Site 1 allowed investigating regulatory capabilities of *B. europaea* under seawater pH values matching the average of the present-day

global surface ocean (IPCC, 2014). In these conditions, $\delta^{11}B$ evaluation showed pH values in the calcifying fluid (pH_{cf}) 0.2–0.4 units above seawater values, DIC_{cf}/DIC_{sw} ratio ranging between ∼1.1 and ∼1.6, and aragonite saturation state Ω_{cf} about 2–4 times higher than that of seawater. Previous studies investigating calcifying fluid pH and carbonate chemistry using geochemical proxies have been conducted mostly on tropical corals and only one investigation was performed on a Mediterranean zooxanthellate colonial coral, *Cladocora caespitosa*, on specimens kept under controlled conditions in aquaria and transplanted at a CO_2 vent (Trotter et al., 2011). This is the first study investigating internal calcifying fluid pH and carbonate chemistry on a Mediterranean coral species exposed to reduced mean seawater aragonite saturation state (Ω_{sw}) for its entire life span. The elevation of pH_{cf} displayed by *B. europaea* falls within reported values for temperate, tropical, and cold-water corals (8.2–8.9) (Trotter et al., 2011; McCulloch et al., 2012b; Wall et al., 2019), yet it was lower than that reported for the temperate coral *C. caespitosa* from the Tyrrhenian Sea (∼8.7) (Trotter et al., 2011), and higher than that of *Porites* spp. from Papua New Guinea (∼8.2) (Wall et al., 2016) and other tropical species (Venn et al., 2013), supporting the hypothesis that the thermal regime is an important driver of pH_{cf} regulation (Trotter et al., 2011; Anagnostou et al., 2012; Ross et al., 2019). Being sympatric species, *B. europaea* and *C. caespitosa* have a widely overlapping habitat distribution; hence, other factors besides acclimation to different thermal environments should be considered when interpreting the observed species-specific pH_{cf} regulation. For example, *B. europaea* and *C. caespitosa* displayed different stress-related transcriptional responses in relation to their peculiar life history traits, symbiotic partnerships, and morphologies (Franzellitti et al., 2018). The same environmental and physiological constraints could affect their degree of biological control over calcification, as previously observed in tropical species (Trotter et al., 2011; Venti et al., 2014; Raybaud et al., 2017). *B. europaea* seems less efficient in up-regulating DIC_{cf} than the tropical corals investigated so far (e.g., *Acropora yongei*: ∼ 3900–4100 μmol kg^{-1}, *Pocillopora damicornis*: ∼3500–3800 μmol kg^{-1}) (Comeau et al., 2017a; McCulloch et al., 2017; Schoepf et al., 2017; Ross et al., 2019). This may have direct implications on the calcification process. Indeed, the ability to regulate DIC_{cf} affects the control of aragonite saturation state Ω_{cf}; thus, it may alter coral ability to buffer calcification changes driven by unfavorable environmental conditions (Cai et al., 2016; McCulloch et al., 2017; Schoepf et al., 2017).

Life-long acclimatization of *B. europaea* polyps to low pH_{TS} conditions as those experienced at Sites 2 and 3 had no apparent effects on average $\delta^{11}B$ and B/Ca, despite the overall 0.33 units change in seawater pH_{TS}. As a result, inferred pH_{cf} and DIC_{cf} values were similar at the different pH_{TS} conditions. It may be hypothesized that under life-long acclimation to altered pH_{TS}, influence of pH_{TS} on inferred DIC_{cf} composition may be negligible. Overall, these results suggest that *B. europaea* is capable of buffering the potentially adverse conditions deriving from persistently living at pH_{TS} values as low as those projected for 2100 (IPCC, 2014) by homeostatically maintaining its physiological pH_{cf}, regardless of external pH_{TS}. pH_{cf} homeostasis under an average seawater pH_{TS} as low as 7.7 has been shown for tropical coral species *Porites cylindrica* and massive *Porites* (Georgiou et al., 2015; Wall et al., 2016) and such ability is now reported in a temperate coral from the Mediterranean Sea. As a further support, a study reporting whole-transcriptome responses of *B. europaea* to combined elevated temperature and low pH_{TS} (7.8) conditions in aquaria showed that stress response in this species largely relies on modulation of metabolic related transcripts, which aid in maintaining physiological homeostasis (Maor-Landaw et al., 2017).

Gross and Net Calcification Rates

By applying a modeling approach that uses pH_{cf}, $CO_3^{2-}{}_{cf}$, and DIC_{cf} (IpHRAC model: McCulloch et al., 2012a), we inferred the aragonite saturation state of the calcifying fluid (Ω_{cf}) and derived GCR, as geochemical proxy data are likely to reflect the micro-scale calcification conditions. These parameters were unaffected by seawater pH_{TS} suggesting that changes of seawater pH_{TS} have a minor impact on calcification processes of *B. europaea*. The homogeneous GCR and micro-NCR (**Figure 5**) found in this study are in line with previous observations on the same specimens which found no changes at the nano and micro-scales in the biomineral polymorph, organic matrix content, aragonite fiber thickness, hardness and density (i.e., micro-density) along the gradient. This suggested that the biomineralization process produced fundamental unitary components of the coral skeleton (the solid matrix, excluding the pores) named "building blocks," with actual features substantially unaffected by decreased seawater pH_{TS}. Fantazzini et al., 2015 hypothesized that the decrease in bulk-NCR (named NCR in that paper) at the low pH sites could be the result of less "building blocks" being produced with increased acidification. The pH up-regulation observed in this study could provide a potential explanation to this hypothesis: if, for simplicity, we compare a single calicoblastic cell (**Figure 6**) in Site 1 (average pH_{TS} = 8.1) and in Site 3 (average pH_{TS} = 7.7), the latter likely needs to work more compared to Site 1 given the larger ΔpH, which also means that it will likely consume more energy. However, if we assume that the available energy is the same at the three sites, in order to provide more energy to cell in Site 3, less calicoblastic cells may be activated as a means to re-allocate the available energy. Thus, where calicoblastic cells are "shut down" no biomineral deposition (i.e., "building block" production) can take place, ultimately leading to the formation of skeletal pores and reduced net calcification (i.e., bulk-NCR) (as summarized in **Figure 6**). It must be noted that besides calcification, the control of intracellular pH is needed to maintain further physiological processes in invertebrates, for example osmoregulation, metabolism and reproductive output (Mayfield and Gates, 2007; Byrne, 2012). Thus, the observed pH homeostasis may contributes to maintaining unchanged reproductive output reported in *B. europaea* along this gradient (Caroselli et al., 2019).

Calcification may be mediated by, or have an influence on, other aspects of the calcifying fluid other than pH_{cf}, $CO_3^{2-}{}_{cf}$, and DIC_{cf}. More specifically, the calcifying fluid calcium ion concentrations can deviate from seawater concentrations

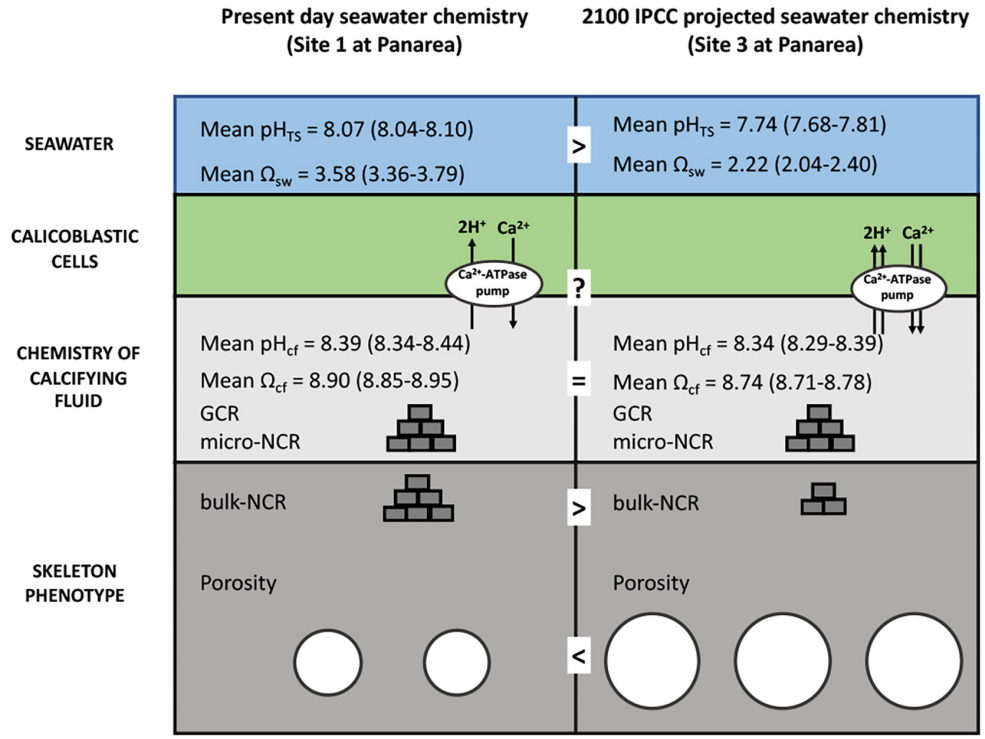

FIGURE 6 | Schematic summary showing the hypothesized impacts of life-long acclimation to low pH on skeletal growth in *Balanophyllia europaea* along the gradient of Panarea. At the current seawater pH (Site 1), *B. europaea* up-regulates pH and carbonate chemistry of the calcifying fluid compared to seawater levels. At low pH_{TS} as those projected for 2100 (Site 3), seawater acidification did not significantly affect pH_{cf} and DIC_{cf}, showing comparable values to those of Site 1. Under these conditions, the bio-inorganic model projects no changes of aragonite saturation state (Ω_{cf}), thus unmodified GCR and micro-NCR, compared to present-day conditions (Site 1), suggesting that *B. europaea* performs an effective biological control over the calcification process. Nevertheless, with increased energy expenditure which is likely needed to maintain calcification, *B. europaea* changes its skeleton phenotype to a morphology characterized by decreased bulk density and increased porosity at the macro-scale, and reduced (measured) bulk-NCR, while maintaining unchanged linear extension rates (Fantazzini et al., 2015). No increases in production of organic matrix proteins (OM) per unit mass of $CaCO_3$ are observed (Fabry et al., 2008). We postulate a tradeoff in energetic balance in which internal carbonate chemistry is homeostatically compensated at the expenses of calicoblastic cell and organic matrix functioning/organization and macro-scale skeleton structure to maintained coral growth (i.e., linear extension rates) and the reproductive output (Andersson and Mackenzie, 2012; Fantazzini et al., 2015).

(e.g., due to species variability, changing rates of calcification on sub-annual timescales) and can therefore mediate Ω_{cf} together with $[CO_3^{2-}]_{cf}$ (Ross et al., 2019). Also, changes in B/Ca derived carbonate ion concentrations in the calcifying fluid are not necessarily equivalent to changes in Ω_{cf} (DeCarlo et al., 2018). This should be cautiously considered when using the IpHRAC model as a framework to compare how bio-calcification rates might deviate from the expected abiotic rate kinetics of aragonite (Burton and Walter, 1987).

Trade-offs among the different biological processes controlling coral physiology (Rippe et al., 2018) may also contribute to explaining the observed decline in bulk-NCR while maintaining unchanged GCR. For example, impaired expression of transcripts underscoring transport mechanisms and organic matrix structure and function (i.e., galaxins, SCRiPs or Small Cysteine-Rich Proteins, collagens) were observed at low pH in different coral species (Moya et al., 2012; Vidal-Dupiol et al., 2013; Kaniewska et al., 2015; Zoccola et al., 2016). Nevertheless, expression of transporters for $[Ca^{2+}]$, $[HCO_3^-]$, or $[H^+]$ ions were unaffected by the acute exposure of the early life stages of *Acropora millepora* to OA conditions (pH = 7.96 and 7.86), while overall reduced expression of transcripts encoding proteins of the skeletal organic matrix was also observed (Moya et al., 2012). These effects may, at least partially, reflect the possible diversion of energy away from $CaCO_3$ deposition toward other physiological processes such as maintenance of pH_{cf} homeostasis (Moya et al., 2012; Georgiou et al., 2015). Therefore, we can hypothesize that a reduced availability of metabolic CO_2 for calcification and less-controlled (or cease of) aragonite precipitation may occur also under pH_{cf} homeostatic control, underpinning the detrimental effects observed on the skeletal macro-structures (Goffredo et al., 2014; Fantazzini et al., 2015). The recent evidences on the role of ACC nanoparticles as precursor of biomineral formation in *S. pistillata* (Von Euw et al., 2017; Drake et al., 2018) suggest the putative onset of multiple routes of calcification in *B. europaea* and, more generally in corals, as already observed in other marine calcifying organisms (Vidavsky et al., 2016; Ramesh et al., 2017). Further analyses to characterize the molecular mediators operating on calcification and organic matrix organization are needed to conclusively address the specific processes occurring in *B. europaea* under short-term and long-term exposure to low seawater pH_{TS}.

Increase of dissolution at the low pH_{TS} Sites could also provide an additional explanation to the reduction in NCRs and increased skeletal porosity found in *B. europaea* along this pH gradient (Fantazzini et al., 2015). Supporting this hypothesis, aragonite saturation in seawater at Site 3 reaches minimum values of 0.4 (**Supplementary Table 1**) leading to transient under-saturated conditions (Goffredo et al., 2014; Prada et al., 2017). Dissolution was also hypothesized by Comeau et al. (2017a) in *A. yongei* to explain the observed strong decrease of NCRs accompanied by a limited decrease of pH_{cf}. In particular, the authors hypothesized possible dissolution at night when dark calcification could be suppressed at low pH_{TS} (Schneider and Erez, 2006). On the other hand, during daytime, relatively high calcification rates and pH_{cf} are maintained by symbiont pCO_2-enhanced photosynthesis (Gattuso et al., 1999). Night-time net dissolution has been previously observed in *A. millepora* by using total alkalinity measurements (Strahl et al., 2015). Thus, the isotopic composition of the skeleton should mostly represent conditions in the calcifying fluid during the day, which could explain the homogeneous internal carbonate chemistry regardless of seawater pH_{TS}.

CONCLUSION

Using a dual geochemical proxy approach, for the first time pH_{cf} and internal carbonate chemistry have been investigated in the temperate zooxanthellate coral *B. europaea* growing for its entire life along a natural pH gradient, thus inferring the impacts of long-term acclimation and the degree of physiological plasticity toward OA. We showed that *B. europaea* exerts an active biological control that allows pH_{cf} and carbonate chemistry homeostasis in the calcifying fluid, ultimately leading to homogeneous modeled GCRs. These results are in agreement with previous observations showing that the features of the "building blocks" produced by the biomineralization process were substantially unaffected by decreased seawater pH_{TS}. It was hypothesized that in order to maintain calcifying fluid homeostasis, *B. europaea* may re-allocate available energy (which we assume is the same along the gradient) toward fewer but more energy-consuming calicoblastic cells at the low pH site. Where calicoblastic cells are not activated, no biomineral precipitation can take place which could lead to the formation of pores and ultimately to the observed decline in NCRs. However, we cannot exclude that the observed response of *B. europaea* along this gradient may be a combination of this and other factors (e.g., dissolution, expression of transporters for $[Ca^{2+}]$, $[HCO_3^-]$, or $[H^+]$ ions, down-regulation of transcripts encoding proteins of the skeletal organic matrix) which likely act in synergy. Further analyses on molecular mediators and organic matrix composition and functioning, which could be likely impaired under environmental changes, as well as direct measurements of gross calcification are needed to shed light on the biomineralization processes occurring in *B. europaea* under low seawater pH_{TS}. Additional studies like the one presented here should be performed on other species and locations to predict whether temperate Mediterranean corals will thrive under projected scenarios of anthropogenic global change.

DATA AVAILABILITY STATEMENT

All data are available from the corresponding authors upon request.

AUTHOR CONTRIBUTIONS

SG, ZD, and GF conceived and designed the research. FP, SG, and EC collected the specimens and provided the background data. MW and JF analyzed the samples. MW, FP, EC, and PM performed the statistical analyses. MW, FP, and SF wrote the first draft. FP, EC, LB, PF, SF, PM, GF, and SG contributed to the scientific discussion and interpretation of the data. All authors contributed to writing the manuscript and gave final approval for publication.

FUNDING

The research leading to these results was supported by the European Research Council under the European Union's Seventh Framework Programme (FP7/2007-2013)/ERC grant agreement number (249930- CoralWarm: Corals and global warming: the Mediterranean versus the Red Sea). EC was supported by the ALMA IDEA grant of the University of Bologna for the project "STRAMICRO." MW was supported by the Austrian Science fund (FWF), Schrödinger Fellowship J-3667: *pH up-regulation in tropical corals: a key mechanism? Implications for the future and the past.*

SUPPLEMENTARY MATERIAL

The Supplementary Material for this article can be found online at: https://www.frontiersin.org/articles/10.3389/fmars.2019.00699/full#supplementary-material

REFERENCES

Allemand, D., Ferrier-Pagès, C., Furla, P., Houlbrèque, F., Puverel, S., Reynaud, S., et al. (2004). Biomineralisation in reef-building corals: from molecular mechanisms to environmental control. *C. R. Palevol* 3, 453–467. doi: 10.1016/j.crpv.2004.07.011

Anagnostou, E., Huang, K. F., You, C. F., Sikes, E. L., and Sherrell, R. M. (2012). Evaluation of boron isotope ratio as a pH proxy in the deep sea coral *Desmophyllum dianthus*: evidence of physiological pH adjustment. *Earth Planet. Sci. Lett.* 34, 251–260. doi: 10.1016/j.epsl.2012.07.006

Andersson, A. J., and Mackenzie, F. T. (2012). Revisiting four scientific debates in ocean acidification research. *Biogeosciences* 9, 893–905. doi: 10.5194/bg-9-893-2012

Beaufort, L., Probert, I., De Garidel-Thoron, T., Bendif, E. M., Ruiz-Pino, D., Metzl, N., et al. (2011). Sensitivity of coccolithophores to carbonate chemistry and ocean acidification. *Nature* 476, 80–83. doi: 10.1038/nature10295

Bucher, D. J., Harriott, V. J., and Roberts, L. G. (1998). Skeletal micro-density, porosity and bulk density of acroporid corals. *J. Exp. Mar. Bio. Ecol.* 228, 117–136. doi: 10.1016/S0022-0981(98)00020-3

Burton, E. A., and Walter, L. M. (1987). Relative precipitation rates of aragonite and Mg calcite from seawater: temperature or carbonate ion control? *Geology* 15, 111–114.

Byrne, M. (2012). Global change ecotoxicology: identification of early life history bottlenecks in marine invertebrates, variable species responses and variable experimental approaches. *Mar. Environ. Res.* 76, 3–15. doi: 10.1016/j.marenvres.2011.10.004

Cai, W. J., Ma, Y., Hopkinson, B. M., Grottoli, A. G., Warner, M. E., Ding, Q., et al. (2016). Microelectrode characterization of coral daytime interior pH and carbonate chemistry. *Nat. Commun.* 7:11144. doi: 10.1038/ncomms11144

Caroselli, E., Gizzi, F., Prada, F., Marchini, C., Airi, V., Kaandorp, J., et al. (2019). Low and variable pH decreases recruitment efficiency in populations of a temperate coral naturally present at a CO_2 vent. *Limnol. Oceanogr.* 64, 1059–1069. doi: 10.1002/lno.11097

Caroselli, E., Pasquini, L., Levy, O., Goffredo, S., Zaccanti, F., Falini, G., et al. (2011). Environmental implications of skeletal micro-density and porosity variation in two scleractinian corals. *Zoology* 114, 255–264. doi: 10.1016/j.zool.2011.04.003

Carricart-Ganivet, J. P. (2004). Sea surface temperature and the growth of the West Atlantic reef-building coral *Montastrea annularis*. *J. Exp. Mar. Bio. Ecol.* 302, 249–260. doi: 10.1016/j.jembe.2003.10.015

Cohen, A., and Holcomb, M. (2009). Why corals care about ocean acidification: uncovering the mechanism. *Oceanography* 22, 118–127. doi: 10.5670/oceanog.2009.102

Cohen, S., and Fine, M. (2012). Measuring gross and net calcification of a reef coral under ocean acidification conditions: methodological considerations. *Biogeosciences Discuss.* 9, 8241–8272. doi: 10.5194/bgd-9-8241-2012

Cohen, S., Krueger, T., and Fine, M. (2017). Measuring coral calcification under ocean acidification: methodological considerations for the ^{45}Ca-uptake and total alkalinity anomaly technique. *PeerJ* 5:e3749. doi: 10.7717/peerj.3749

Comeau, S., Cornwall, C. E., and McCulloch, M. T. (2017a). Decoupling between the response of coral calcifying fluid pH and calcification to ocean acidification. *Sci. Rep.* 7, 7573. doi: 10.1038/s41598-017-08003-z

Comeau, S., Tambutté, E., Carpenter, R. C., Edmunds, P. J., Evensen, N. R., Allemand, D., et al. (2017b). Coral calcifying fluid pH is modulated by seawater carbonate chemistry not solely seawater pH. *Proc. R. Soc. B Biol. Sci.* 284:20161669. doi: 10.1098/rspb.2016.1669

Comeau, S., Edmunds, P. J., Spindel, N. B., and Carpenter, R. C. (2014). Fast coral reef calcifiers are more sensitive to ocean acidification in short-term laboratory incubations. *Limnol. Ocean.* 59, 1081–1091. doi: 10.4319/lo.2014.59.3.1081

Connell, S. D., and Russell, B. D. (2010). The direct effects of increasing CO_2 and temperature on non-calcifying organisms: increasing the potential for phase shifts in kelp forests. *Proc. R. Soc. B Biol. Sci.* 277, 1409–1415. doi: 10.1098/rspb.2009.2069

De'ath, G., Lough, J. M., and Fabricius, K. E. (2009). Declining coral calcification on the great barrier reef. *Science* 323, 116–119. doi: 10.1126/science.1165283

DeCarlo, T. M., Comeau, S., Cornwall, C. E., and McCulloch, M. T. (2018). Coral resistance to ocean acidification linked to increased calcium at the site of calcification. *Proc. R. Soc. B Biol. Sci.* 285:20180564. doi: 10.1098/rspb.2018.0564

DeCarlo, T. M., D'Olivo, J. P., Foster, T., Holcomb, M., Becker, T., and McCulloch, M. T. (2017). Coral calcifying fluid aragonite saturation states derived from Raman spectroscopy. *Biogeosciences* 14, 5253–5269. doi: 10.5194/bg-14-5253-2017

Dickson, A. G. (1990). Standard potential of the reaction: $AgCl(s) + 12H_2(g) = Ag(s) + HCl(aq)$ and the standard acidity constant of the ion HSO_4^- in synthetic seawater from 273.15 to 318.15 K. *J. Chem. Thermodyn.* 22, 113–127. doi: 10.1016/0021-9614(90)90074-z

Drake, J. L., Schaller, M. F., Mass, T., Godfrey, L., Fu, A., Sherrell, R. M., et al. (2018). Molecular and geochemical perspectives on the influence of CO_2 on calcification in coral cell cultures. *Limnol. Oceanogr.* 63, 107–212. doi: 10.1002/lno.10617

Eyre, B. D., Cyronak, T., Drupp, P., De Carlo, E. H., Sachs, J. P., and Andersson, A. J. (2018). Coral reefs will transition to net dissolving before end of century. *Science* 359, 908–911. doi: 10.1126/science.aao1118

Fabricius, K. E., Langdon, C., Uthicke, S., Humphrey, C., Noonan, S., De'ath, G., et al. (2011). Losers and winners in coral reefs acclimatized to elevated carbon dioxide concentrations. *Nat. Clim. Chang.* 1, 165–169. doi: 10.1038/nclimate1122

Fabry, V. J., Seibel, B. A., Feely, R. A., and Orr, J. C. (2008). Impacts of ocean acidification on marine fauna and ecosystem processes. *ICES J. Mar. Sci.* 65, 414–432. doi: 10.1093/icesjms/fsn048

Fantazzini, P., Mengoli, S., Pasquini, L., Bortolotti, V., Brizi, L., Mariani, M., et al. (2015). Gains and losses of coral skeletal porosity changes with ocean acidification acclimation. *Nat. Commun.* 6:8785. doi: 10.1038/ncomms8785

Fietzke, J., Heinemann, A., Taubner, I., Böhm, F., Erez, J., and Eisenhauer, A. (2010). Boron isotope ratio determination in carbonates via LA-MC-ICP-MS using soda-lime glass standards as reference material. *J. Anal. At. Spectrom.* 25, 1953–1957. doi: 10.1039/c0ja00036a

Foster, G. L., Pogge von Strandmann, P. A. E., and Rae, J. W. B. (2010). Boron and magnesium isotopic composition of seawater. *Geochemistry, Geophys. Geosystems* 11:Q08015. doi: 10.1029/2010GC003201

Franzellitti, S., Airi, V., Calbucci, D., Caroselli, E., Prada, F., Voolstra, C. R., et al. (2018). Transcriptional response of the heat shock gene hsp70 aligns with differences in stress susceptibility of shallow-water corals from the Mediterranean Sea. *Mar. Environ. Res.* 140, 444–454. doi: 10.1016/j.marenvres.2018.07.006

Gabriel, K. R., and Lachenbruch, P. A. (1969). Non-parametric ANOVA in small samples: a Monte Carlo study of the adequacy of the asymptotic approximation. *Biometrics* 25, 539–596.

Gagnon, A. C., Adkins, J. F., and Erez, J. (2012). Seawater transport during coral biomineralization. *Earth Planet. Sci. Lett.* 329–330, 150–161. doi: 10.1016/j.epsl.2012.03.005

Gattuso, J.-P., Allemand, D., and Frankignoulle, M. (1999). Photosynthesis and calcification at cellular, organismal and community levels in coral reefs: a review on interactions and control by carbonate chemistry. *Am. Zool.* 39, 160–183. doi: 10.1093/icb/39.1.160

Gazeau, F., Parker, L. M., Comeau, S., Gattuso, J.-P., O'Connor, W. A., Martin, S., et al. (2013). Impacts of ocean acidification on marine shelled molluscs. *Mar. Biol.* 160, 2207–2245. doi: 10.1007/s00227-013-2219-3

Georgiou, L., Falter, J., Trotter, J., Kline, D. I., Holcomb, M., Dove, S. G., et al. (2015). pH homeostasis during coral calcification in a free ocean CO_2 enrichment (FOCE) experiment, Heron Island reef flat, Great Barrier Reef. *Proc. Natl. Acad. Sci. U.S.A.* 112, 13219–13224. doi: 10.1073/pnas.1505586112

Goffredo, S., Prada, F., Caroselli, E., Capaccioni, B., Zaccanti, F., Pasquini, L., et al. (2014). Biomineralization control related to population density under ocean acidification. *Nat. Clim. Chang.* 4, 593–597. doi: 10.1038/nclimate2241

Hemming, N. G., and Hanson, G. N. (1992). Boron isotopic composition and concentration in modern marine carbonates. *Geochim. Cosmochim. Acta* 56, 537–543. doi: 10.1016/0016-7037(92)90151-8

Holcomb, M., DeCarlo, T. M., Gaetani, G. A., and McCulloch, M. (2016). Factors affecting B/Ca ratios in synthetic aragonite. *Chem. Geol.* 437, 67–76. doi: 10.1016/j.chemgeo.2016.05.007

Hönisch, B., Hemming, N. G., Grottoli, A. G., Amat, A., Hanson, G. N., and Bijma, J. (2004). Assessing scleractinian corals as recorders for paleo-pH: empirical calibration and vital effects. *Geochim. Cosmochim. Acta.* 68, 3675–3685. doi: 10.1016/j.gca.2004.03.002

IPCC (2014). *Climate Change 2014: Synthesis Report. Contribution of Working Groups I, II and III to the Fifth Assessment Report of the Intergovernmental Panel on Climate Change*. Geneva: IPCC.

Kaniewska, P., Chan, C. K. K., Kline, D., Ling, E. Y. S., Rosic, N., Edwards, D., et al. (2015). Transcriptomic changes in coral holobionts provide insights into physiological challenges of future climate and ocean change. *PLoS One* 10:e0139223. doi: 10.1371/journal.pone.0139223

Klochko, K., Kaufman, A. J., Yao, W., Byrne, R. H., and Tossell, J. A. (2006). Experimental measurement of boron isotope fractionation in seawater. *Earth Planet. Sci. Lett.* 248, 276–285. doi: 10.1016/j.epsl.2006.05.034

Krief, S., Hendy, E. J., Fine, M., Yam, R., Meibom, A., Foster, G. L., et al. (2010). Physiological and isotopic responses of scleractinian corals to ocean

acidification. *Geochim. Cosmochim. Acta* 74, 4988–5001. doi: 10.1016/j.gca.2010.05.023

Lough, J. M., and Barnes, D. J. (2000). Environmental controls on growth of the massive coral Porites. *J. Exp. Mar. Bio. Ecol.* 245, 225–243. doi: 10.1016/S0022-0981(99)00168-9

Maor-Landaw, K., Waldman Ben-Asher, H., Karako-Lampert, S., Salmon-Divon, M., Prada, F., Caroselli, E., et al. (2017). Mediterranean versus Red sea corals facing climate change, a transcriptome analysis. *Sci. Rep.* 7, 3–10. doi: 10.1038/srep42405

Mass, T., Giuffre, A. J., Sun, C.-Y., Stifler, C. A., Frazier, M. J., Neder, M., et al. (2017). Amorphous calcium carbonate particles form coral skeletons. *Proc. Natl. Acad. Sci. U.S.A.* 114, E7670–E7678. doi: 10.1073/pnas.1707890114

Mayfield, A. B., and Gates, R. D. (2007). Osmoregulation in anthozoan-dinoflagellate symbiosis. *Comp. Biochem. Physiol. A Mol. Integr. Physiol.* 147, 1–10. doi: 10.1016/j.cbpa.2006.12.042

McCulloch, M., Falter, J., Trotter, J., and Montagna, P. (2012a). Coral resilience to ocean acidification and global warming through pH up-regulation. *Nat. Clim. Chang.* 2, 623–627. doi: 10.1038/nclimate1473

McCulloch, M., Trotter, J., Montagna, P., Falter, J., Dunbar, R., Freiwald, A., et al. (2012b). Resilience of cold-water scleractinian corals to ocean acidification: Boron isotopic systematics of pH and saturation state up-regulation. *Geochim. Cosmochim. Acta* 87, 21–34. doi: 10.1016/j.gca.2012.03.027

McCulloch, M. T., D'Olivo, J. P., Falter, J., Georgiou, L., Holcomb, M., Montagna, P., et al. (2018). "Boron Isotopic Systematics in Scleractinian Corals and the Role of pH Up-regulation," in *Boron Isotopes: The Fifth Element: Advances in Isotope Geochemistry*, eds H. Marschall, and G. Foster, (Cham: Springer International Publishing AG), 145–162. doi: 10.1007/978-3-319-64666-4_6

McCulloch, M. T., D'Olivo, J. P., Falter, J., Holcomb, M., and Trotter, J. A. (2017). Coral calcification in a changing world and the interactive dynamics of pH and DIC upregulation. *Nat. Commun.* 8:15686. doi: 10.1038/ncomms15686

Miller, G. M., Watson, S. A., Mccormick, M. I., and Munday, P. L. (2013). Increased CO_2 stimulates reproduction in a coral reef fish. *Glob. Chang. Biol.* 19, 3037–3045. doi: 10.1111/gcb.12259

Millero, F. J., Graham, T. B., Huang, F., Bustos-Serrano, H., and Pierrot, D. (2006). Dissociation constants of carbonic acid in seawater as a function of salinity and temperature. *Mar. Chem.* 100, 80–94. doi: 10.1016/j.marchem.2005.12.001

Moya, A., Huisman, L., Ball, E. E., Hayward, D. C., Grasso, L. C., Chua, C. M., et al. (2012). Whole transcriptome analysis of the coral *Acropora millepora* reveals complex responses to CO_2-driven acidification during the initiation of calcification. *Mol. Ecol.* 21, 2440–2454. doi: 10.1111/j.1365-294X.2012.05554.x

Ohno, Y., Iguchi, A., Shinzato, C., Inoue, M., Suzuki, A., Sakai, K., et al. (2017). An aposymbiotic primary coral polyp counteracts acidification by active pH regulation. *Sci. Rep.* 7:40324. doi: 10.1038/srep40324

Prada, F., Caroselli, E., Mengoli, S., Brizi, L., Fantazzini, P., Capaccioni, B., et al. (2017). Ocean warming and acidification synergistically increase coral mortality. *Sci. Rep.* 7:40842. doi: 10.1038/srep40842

R Core Team (2015). *R: A Language and Environment for Statistical Computing*. Vienna, Austria: R Foundation for Statistical Computing. Available at: https://cran.r-project.org/.

Ramesh, K., Hu, M. Y., Thomsen, J., Bleich, M., and Melzner, F. (2017). Mussel larvae modify calcifying fluid carbonate chemistry to promote calcification. *Nat. Commun.* 8:1709. doi: 10.1038/s41467-017-01806-8

Raybaud, V., Tambutté, S., Ferrier-Pagès, C., Reynaud, S., Venn, A. A., Tambutté, É, et al. (2017). Computing the carbonate chemistry of the coral calcifying medium and its response to ocean acidification. *J. Theor. Biol.* 424, 26–36. doi: 10.1016/j.jtbi.2017.04.028

Ries, J. B., Cohen, A. L., and McCorkle, D. C. (2009). Marine calcifiers exhibit mixed responses to CO_2-induced ocean acidification. *Geology* 37, 1131–1134. doi: 10.1130/G30210A.1

Rippe, J. P., Baumann, J. H., De Leener, D. N., Aichelman, H. E., Friedlander, E. B., Davies, S. W., et al. (2018). Corals sustain growth but not skeletal density across the Florida Keys Reef Tract despite ongoing warming. *Glob. Chang. Biol.* 24, 5205–5217. doi: 10.1111/gcb.14422

Rodolfo-Metalpa, R., Houlbrèque, F., Tambutté, É, Boisson, F., Baggini, C., Patti, F. P., et al. (2011). Coral and mollusc resistance to ocean acidification adversely affected by warming. *Nat. Clim. Change* 1, 308–312. doi: 10.1038/nclimate1200

Ross, C. L., DeCarlo, T. M., and McCulloch, M. T. (2019). Environmental and physiochemical controls on coral calcification along a latitudinal temperature gradient in Western Australia. *Glob. Chang. Biol.* 25, 431–447. doi: 10.1111/gcb.14488

Schneider, K., and Erez, J. (2006). The effect of carbonate chemistry on calcification and photosynthesis in the hermatypic coral *Acropora eurystoma*. *Limnol. Oceanogr.* 51, 1284–1293. doi: 10.4319/lo.2006.51.3.1284

Schoepf, V., Jury, C. P., Toonen, R. J., and McCulloch, M. T. (2017). Coral calcification mechanisms facilitate adaptive responses to ocean acidification. *Proc. Biol. Sci.* 284:20172117. doi: 10.1098/rspb.2017.2117

Sevilgen, D. S., Venn, A. A., Hu, M. Y., Tambutté, E., de Beer, D., Planas-Bielsa, V., et al. (2019). Full *in vivo* characterization of carbonate chemistry at the site of calcification in corals. *Sci. Adv.* 5:eaau7447. doi: 10.1126/sciadv.aau7447

Smith, S. V., and Key, G. S. (1975). Carbon dioxide and metabolisn˜ in marine environments1. *Limnol. Oceangr.* 20, 493–495. doi: 10.4319/lo.1975.20.3.0493

Strahl, J., Stolz, I., Uthicke, S., Vogel, N., Noonan, S. H. C., and Fabricius, K. E. (2015). Physiological and ecological performance differs in four coral taxa at a volcanic carbon dioxide seep. *Comp. Biochem. Physiol. Part A Mol. Integr. Physiol.* 184, 179–186. doi: 10.1016/j.cbpa.2015.02.018

Tortolero-Langarica, J. D. J. A., Rodríguez-Troncoso, A. P., Cupul-Magaña, A. L., and Carricart-Ganivet, J. P. (2017). Calcification and growth rate recovery of the reef-building *Pocillopora* species in the northeast tropical Pacific following an ENSO disturbance. *PeerJ* 5:e3191. doi: 10.7717/peerj.3191

Trotter, J., Montagna, P., McCulloch, M., Silenzi, S., Reynaud, S., Mortimer, G., et al. (2011). Quantifying the pH 'vital effect' in the temperate zooxanthellate coral *Cladocora caespitosa*: validation of the boron seawater pH proxy. *Earth Planet. Sci. Lett.* 303, 163–173. doi: 10.1016/j.epsl.2011.01.030

Venn, A. A., Tambutte, E., Holcomb, M., Laurent, J., Allemand, D., and Tambutte, S. (2013). Impact of seawater acidification on pH at the tissue-skeleton interface and calcification in reef corals. *Proc. Natl. Acad. Sci. U.S.A.* 110, 1634–1639. doi: 10.1073/pnas.1216153110

Venti, A., Andersson, A., and Langdon, C. (2014). Multiple driving factors explain spatial and temporal variability in coral calcification rates on the Bermuda platform. *Coral Reefs* 33, 979–997. doi: 10.1007/s00338-014-1191-9

Vidal-Dupiol, J., Zoccola, D., Tambutté, E., Grunau, C., Cosseau, C., Smith, K. M., et al. (2013). Genes related to ion-transport and energy production are upregulated in response to CO_2-driven pH decrease in corals: new insights from transcriptome analysis. *PLoS One* 8:e58652. doi: 10.1371/journal.pone.0058652

Vidavsky, N., Addadi, S., Schertel, A., Ben-Ezra, D., Shpigel, M., Addadi, L., et al. (2016). Calcium transport into the cells of the sea urchin larva in relation to spicule formation. *Proc. Natl. Acad. Sci. U.S.A.* 113, 12637–12642. doi: 10.1073/pnas.1612017113

Von Euw, S., Zhang, Q., Manichev, V., Murali, N., Gross, J., Feldman, L. C., et al. (2017). Biological control of aragonite formation in stony corals. *Science* 356, 933–938. doi: 10.1126/science.aam6371

Wall, M., Fietzke, J., Crook, E. D., and Paytan, A. (2019). Using B isotopes and B/Ca in corals from low saturation springs to constrain calcification mechanisms. *Nat. Commun.* 10:3580. doi: 10.1038/s41467-019-11519-9

Wall, M., Fietzke, J., Schmidt, G. M., Fink, A., Hofmann, L. C., de Beer, D., et al. (2016). Internal pH regulation facilitates in situ long-term acclimation of massive corals to end-of-century carbon dioxide conditions. *Sci. Rep.* 6:30688. doi: 10.1038/srep30688

Zoccola, D., Ganot, P., Bertucci, A., Caminiti-Segonds, N., Techer, N., Voolstra, C. R., et al. (2015). Bicarbonate transporters in corals point towards a key step in the evolution of cnidarian calcification. *Sci. Rep.* 5:09983. doi: 10.1038/srep09983

Zoccola, D., Innocenti, A., Bertucci, A., Tambutté, E., Supuran, C. T., and Tambutté, S. (2016). Coral carbonic anhydrases: regulation by ocean acidification. *Mar. Drugs.* 14:109. doi: 10.3390/md14060109

Conflict of Interest: The authors declare that the research was conducted in the absence of any commercial or financial relationships that could be construed as a potential conflict of interest.